



# Dynamics of the discrete Seno population model: Combined effects of harvest timing and intensity on population stability



Daniel Franco<sup>a,\*</sup>, Hartmut Logemann<sup>b</sup>, Juan Perán<sup>a</sup>, Juan Segura<sup>a,c</sup>

<sup>a</sup> Departamento de Matemática Aplicada, E.T.S.I. Industriales, Universidad Nacional de Educación a Distancia (UNED), c/ Juan del Rosal 12, 28040, Madrid, Spain

<sup>b</sup> Department of Mathematical Sciences, University of Bath, Bath BA2 7AY, UK

<sup>c</sup> Departament d'Economia i Empresa, Universitat Pompeu Fabra, c/ Ramon Trias Fargas 25–27, 08005, Barcelona, Spain

## ARTICLE INFO

### Article history:

Received 9 August 2016

Revised 17 February 2017

Accepted 22 February 2017

Available online 28 February 2017

### Keywords:

Constant effort harvesting

Discrete population model

Stabilization

Ricker map

Schwarzian derivative

## ABSTRACT

The paper contains new results on the impact of harvesting times and intensities on the stability properties of Seno population models. It is proved that sufficiently high harvest intensities are stabilizing for any harvesting time in the sense that they create a positive equilibrium that attracts all positive solutions. Moreover, in the special case that the nonlinearity in the Seno model is a Ricker function, we derive a global stability result independent of timing and valid for low to medium harvesting efforts. The proof is based on a characterization of those harvesting intensities which guarantee a negative Schwarzian derivative for all harvesting times. Finally, we rigorously show that timing can be stabilizing as well as destabilizing by itself. In particular, a recent conjecture formulated by Cid et al. (2014) [1] is shown to be false.

© 2017 Elsevier Inc. All rights reserved.

## 1. Introduction

The time of intervention in harvesting programmes has been proved to play an important role on the population persistence. This role is especially important in seasonally reproducing species [2–5]. In this sense, harvest timing is currently receiving an increasing attention. However, the existing literature has mostly focused on the population size, see e.g. [3,6], and few studies have analyzed the effects on the population stability.

This motivated Cid et al. [1] to use a model proposed by Seno [7] to study the effect of harvest timing on both the size and stability of populations. Seno's model is given by a single one-dimensional difference equation based on constant effort harvesting (also known as proportional harvesting) that allows for the consideration of any moment during the reproductive season for the intervention. When harvesting occurs at the beginning or at the end of the reproductive period, two topologically conjugated systems are obtained. For these systems, removing individuals can create an asymptotically stable positive equilibrium which acts as a global attractor under certain conditions [8,9]. On the contrary, if the harvesting intensity is too high, populations starting with any initial size go eventually extinct [10]. Interestingly, when individuals are removed at an intermediate moment during the reproductive season, the stability properties of Seno's model are not so well understood.

Cid et al. [1] proved that for any intervention time the system has a unique positive equilibrium if the intervention effort is below a certain threshold. Moreover, the origin acts as a global attractor when that threshold is reached or exceeded.

\* Corresponding author.

E-mail address: [dfranco@ind.uned.es](mailto:dfranco@ind.uned.es) (D. Franco).

Regarding the asymptotic stability of the positive fixed point, they obtain sharp global results for the quadratic map and a sufficient local condition for the Ricker map [11]. This last condition states that the positive equilibrium of the Ricker–Seno model is asymptotically stable for any harvest time if harvesting at the beginning of the reproductive season guarantees stability. These results, together with numerical simulations, lead Cid et al. [1] to conjecture that the sufficient condition proved for the Ricker–Seno model is true for any other population model described by a unimodal map.

In this paper, we show that the moment of the intervention does not affect the stability of controlled populations when the harvesting effort is high. Moreover, we prove that for high removal intensities—below the threshold above which all populations go eventually extinct—the positive equilibrium acts as a global attractor. This result is valid for a wide family of population models described by unimodal maps and, in particular, it implies that the aforementioned conjecture in [1] is true for high harvesting intensities.

From a practical point of view, the global stability of the positive equilibrium is a desirable property since it allows to predict the dynamics with independence of the initial population size. However, choosing a high harvesting intensity close to the threshold above which all populations go eventually extinct has two important drawbacks. First, surpassing this threshold causes the extinction of the population. Thus, selecting harvesting efforts near such a threshold could be considered dangerous. Second, very high harvesting efforts may be difficult to attain in real situations due to constraints of harvesting/thinning management: for example the number of boats available for fishing or the limited effectiveness of a poison used in pest control. This unveils the importance of extending the previous global stability result to lower harvesting intensities. We do it here for the Ricker–Seno model.

The Ricker model has been shown to be a good descriptor of the dynamics of many populations (including bacteria, fungi, ciliates, crustaceans, fruit flies, and fishes [12]), which makes the study of the stability properties of the Ricker–Seno model appealing. Interestingly, in many population models involving the Ricker map local stability implies global stability, e.g. [13–16]. We show that this is also the case for the Ricker–Seno model if we select a low-medium harvesting effort. Hence, we refine the result given in Proposition 3.4 of [1] by determining a range of intervention efforts for which the positive fixed point is not only asymptotically stable but also attracts all positive orbits. Additionally, we use the Ricker–Seno model to prove that timing can be stabilizing by itself. In other words, we show that in some cases choosing an appropriate moment for removing individuals can induce an asymptotically stable positive fixed point in populations for which the same equilibrium would be unstable in case of triggering the intervention at the beginning or at the end on the reproductive season.

Our last result consists in pointing out that timing can be destabilizing for certain maps satisfying the general conditions assumed on population production maps in [1]. We obtain specific mathematical counterexamples proving that the Conjecture 3.5 in [1] is false. Nevertheless, the implications of this destabilizing effect of timing should be considered carefully because most of the populations maps considered in the ecological literature satisfy extra conditions, which could prevent this destabilizing effect to occur.

The paper is organized as follows. In Section 2 we describe Seno's model and collect the conditions assumed on the population models. Section 3 shows that timing does not affect stability for high harvesting efforts. In Section 4 we study the stability properties of the Ricker–Seno model. Moreover, we show that timing can be stabilizing by itself and we introduce biological realities to check the robustness of our results. Section 5 includes counterexamples proving that harvest timing could be destabilizing. Finally, Section 6 summarizes the results obtained and discusses their implications and limitations.

## 2. Harvesting model with timing

Consider the discrete-time single-species population model

$$x_{t+1} = g(x_t)x_t, \quad (1)$$

where  $x_t \in [0, \infty)$  is the population size at the beginning of the reproductive season  $t$  and  $g : [0, \infty) \rightarrow \mathbb{R}$  is the per-capita production function. It is well established that harvesting a constant fraction  $\gamma \in (0, 1)$  of the population at the end of every reproductive season corresponds to multiplication of the right hand side of (1) by the survival fraction  $(1 - \gamma)$ ,

$$x_{t+1} = (1 - \gamma)g(x_t)x_t. \quad (2)$$

On the other hand, harvesting the same fraction at the beginning of the season leads to

$$x_{t+1} = g((1 - \gamma)x_t)(1 - \gamma)x_t, \quad (3)$$

that is, multiplies the population size  $x_t$  by the survival fraction  $(1 - \gamma)$ . As usual in the literature, we refer to parameter  $\gamma$  as harvesting effort or harvesting intensity. Note that harvesting at the beginning of the season corresponds to an application of the proportional feedback chaos control method proposed in [17] to (1).

In [7], Seno puts forward the following harvesting model, which encompasses the *limit* situations (2) and (3) by allowing the population to be harvested at any fixed point in time within the season. It reads

$$x_{t+1} = [\theta g(x_t) + (1 - \theta)g((1 - \gamma)x_t)](1 - \gamma)x_t, \quad (4)$$

where  $\theta \in [0, 1]$  corresponds to the fixed harvesting moment. Model (4) assumes that the reproductive success at the end of the season depends on the amount of energy accumulated during it. Since the per-capita production depends on  $x_t$  before

$\theta$  and on  $(1 - \gamma)x_t$  afterwards, it is natural to assume that the population production is proportional to the time period before/after harvesting to arrive at (4). See [7,18] for a more detailed explanation and a graphical scheme of the population dynamics of this model.

Following the notation of [1], we rewrite the right-hand side of (4) as

$$\theta F_1(x_t) + (1 - \theta)F_0(x_t) := F_\theta(x_t),$$

where  $F_1(x) := (1 - \gamma)g(x)x$  and  $F_0(x) := g((1 - \gamma)x)(1 - \gamma)x$ . For every particular choice of  $\theta \in [0, 1]$  the map  $F_\theta(x)$  is the convex combination of the maps defining (2) and (3). Consequently, model (4) includes models (2) and (3) as special cases. Taking  $\theta = 1$  corresponds to harvesting when the season ends, and  $\theta = 0$  when it begins.

In this paper, we are interested in populations satisfying the following conditions on  $g$ :

- (i)  $g'(x) < 0$  for all  $x > 0$ ;
- (ii)  $g(0) > 1$ ;
- (iii)  $\lim_{x \rightarrow \infty} g(x) = \delta < 1$ ;
- (iv) there exists some  $d > 0$  such that  $xg(x)$  is strictly increasing on  $(0, d)$  and strictly decreasing on  $(d, \infty)$ .

Biologically speaking, condition (i) states that the dynamics is compensatory, i.e., any increase in the population size in a generation is followed by an increase in mortality in the next generation. Condition (ii) is equivalent to  $\frac{d}{dx}(xg(x))(0) > 1$ , which implies that  $xg(x)$  is above  $y = x$  around  $x = 0$ . Therefore, the population grows for small population sizes. Condition (iv) means in particular that  $xg(x)$  is a unimodal map, we note that (iv) implies (iii) with  $\delta = 0$ —here (iii) is introduced just for ease of reference to [1]. With these conditions, the system has two fixed points  $x = 0$  and  $x = K > 0$ , and the asymptotic dynamics is overcompensatory [19]: for  $x$  large, any increase in the population size is exceeded in magnitude by the corresponding increase in mortality in the following generation, and thus the population function  $xg(x)$  decreases.

Overcompensatory models can exhibit positive unstable equilibria, which leads to fluctuating dynamics [20]. Since we are interested in the combined effect of harvesting timing and harvesting effort on the stability properties of the positive equilibrium, we recall a sufficient and necessary condition for the existence of such an equilibrium regardless of the intervention moment  $\theta$ .

**Proposition 1** (from Proposition 3.1 in [1]). *Assume that conditions (i)–(iii) hold. System (4) has a unique positive equilibrium (denoted by  $K_\gamma(\theta)$ ) if and only if*

$$\gamma < \gamma^* := 1 - \frac{1}{g(0)}.$$

### 3. Timing does not affect stability for high harvesting efforts

In this section, we show that the asymptotic stability of  $K_\gamma(0)$  implies the asymptotic stability of  $K_\gamma(\theta)$  for  $\theta \in [0, 1]$  if  $\gamma$  is chosen close enough to  $\gamma^*$  and  $g$  satisfies conditions (i), (ii) and (iv). Moreover, we obtain that  $K_\gamma(\theta)$  is not only asymptotically stable, but attracts all solutions of (4) starting with a positive initial condition.

**Proposition 2.** *Assume that conditions (i), (ii) and (iv) hold. Then, there exists  $\gamma_0 < \gamma^*$  such that for  $\gamma \in [\gamma_0, \gamma^*)$  the fixed point  $K_\gamma(\theta)$  of (4) is asymptotically stable for all  $\theta \in [0, 1]$  and all positive solutions of (4) converge to  $K_\gamma(\theta)$ .*

**Proof.** Our aim is to prove that the fixed point  $K_\gamma(\theta)$  of  $F_\theta$  attracts all positive solutions of (4), provided that  $\gamma$  is sufficiently close to  $\gamma^*$ . We do this by showing that  $x < F_\theta(x) < K_\gamma(\theta)$  for all  $x \in (0, K_\gamma(\theta))$  and  $F_\theta(x) < x$  for all  $x > K_\gamma(\theta)$ ; see [21, Lemma 1].

A simple calculation yields that  $\frac{dF_\theta}{dx}(0) = F'_\theta(0) = (1 - \gamma)g(0)$  and so, by Proposition 1 and condition (ii),  $F'_\theta(0) > 1$  for every  $\theta \in [0, 1]$  and every  $\gamma \in [0, \gamma^*)$ . Together with the uniqueness of the positive fixed point (see Proposition 1) it now follows that

$$F_\theta(x) > x, \quad x \in (0, K_\gamma(\theta)),$$

for every  $\theta \in [0, 1]$  and every  $\gamma \in [0, \gamma^*)$ .

Next, the inequality  $x > F_\theta(x)$  for all  $x > K_\gamma(\theta)$  follows from the uniqueness of the positive fixed point and the fact that, by condition (iv),  $xg(x) < x$  for  $x > K$ . It is then immediate that  $F_\theta(x) = (1 - \gamma)(xg(x)) < (1 - \gamma)x < x$  for  $x > K$ . For  $x$  large enough,  $(1 - \gamma)x > K$ , and thus  $F_1(x) = ((1 - \gamma)x)g((1 - \gamma)x) < (1 - \gamma)x < x$ . This yields  $F_\theta(x) < x$  for large  $x$ .

To finish the proof, we will show that there exists  $\gamma_0 < \gamma^*$  such that  $F_\theta$  is strictly increasing on the interval  $[0, K_\gamma(\theta))$  for  $\gamma \in [\gamma_0, \gamma^*)$ . This combined with  $K_\gamma(\theta)$  being a fixed point of  $F_\theta$  implies, for every  $\theta \in [0, 1]$  and  $\gamma \in [\gamma_0, \gamma^*)$ , that  $F_\theta(x) < K_\gamma(\theta)$  for  $x \in (0, K_\gamma(\theta))$ .

Since  $F'_\theta(x) = F'_1((1 - \gamma)x)$ , the graph of  $F'_\theta$  is the graph of  $F'_1$  horizontally stretched by a factor  $1 - \gamma$ ; see Fig. 1. For  $\gamma < \gamma^*$ , both graphs are above the horizontal axis near  $x = 0$ . Therefore,  $F'_1(x) < F'_\theta(x)$  around  $x = 0$ . On the other hand,  $F'_\theta(x) = \theta F'_1(x) + (1 - \theta)F'_0(x)$ , implying that  $0 < F'_1(x) \leq F'_\theta(x) \leq F'_0(x)$  around  $x = 0$ .

Let  $C_\gamma(\theta)$  denote the first zero of  $F'_\theta$ . Note that this zero exists because  $F_1$  and  $F_0$  inherit the unimodal character of  $xg(x)$  assumed in condition (iv). Indeed, for  $F'_0$  and  $F'_1$  this zero is unique and corresponds to  $C_\gamma(1) = d$  and  $C_\gamma(0) = \frac{d}{1 - \gamma}$ , respectively.

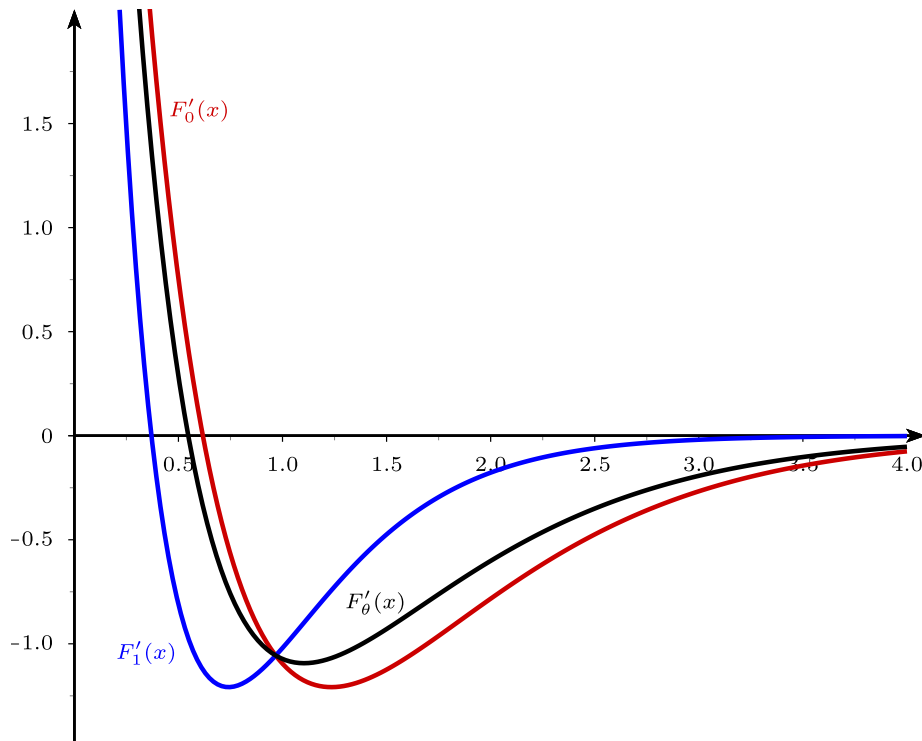


**Fig. 1.** Derivatives of  $F_1$  (blue curve),  $F_0$  (red curve) and  $F'_\theta$  (black curve) when  $g(x) = e^{2.7(1-x)}$ ,  $\gamma = 0.4$  and  $\theta = 0.3$ . (For interpretation of the references to color in this figure legend, the reader is referred to the web version of this article).

From the above discussion, we have that

$$C_\gamma(1) \leq C_\gamma(\theta) \leq C_\gamma(0). \tag{5}$$

We want to find conditions on the parameters guaranteeing that  $F_\theta$  is increasing until  $K_\gamma(\theta)$ , i.e.,  $F'_\theta(x) > 0$  for all  $x < K_\gamma(\theta)$ . This is equivalent to impose  $K_\gamma(\theta) \leq C_\gamma(\theta)$ , and a sufficient condition for this is  $K_\gamma(0) \leq C_\gamma(1)$ . This is true because (5) and Proposition 3.2 in [1] yield  $K_\gamma(\theta) \leq K_\gamma(0) \leq C_\gamma(1) \leq C_\gamma(\theta)$ . Since  $xg(x)$  is increasing on  $(0, d)$ , it follows that the map  $j : [\max\{0, 1 - \frac{1}{g(d)}\}, \gamma^*] \rightarrow [0, g(d)]$  given by  $j(\gamma) = K_\gamma(0)$  is strictly decreasing and satisfies  $\lim_{\gamma \rightarrow \gamma^*} j(\gamma) = 0$ . Hence, there exists a unique  $\gamma_0 \in [\max\{0, 1 - \frac{1}{g(d)}\}, \gamma^*]$  such that  $K_\gamma(0) \leq C_\gamma(1)$  for all  $\gamma \geq \gamma_0$ .

Finally, by construction we have that  $\gamma_0 = 0$  or  $K_{\gamma_0}(0) = C_{\gamma_0}(1) = d$ . Since  $K_{\gamma_0}(0)$  is the unique fixed point of  $F_0$ , then  $\gamma_0$  is the unique solution of

$$g((1 - \gamma_0)d) = \frac{1}{1 - \gamma_0}$$

in the interval  $[\max\{0, 1 - \frac{1}{g(d)}\}, \gamma^*]$ .  $\square$

It is well known that harvesting can induce stability for the positive equilibrium of systems satisfying conditions (i), (ii) and (iv), see e.g. [10]. Proposition 2 provides a threshold  $\gamma_0$  in the removal intensity above which the positive equilibrium becomes a global attractor. The previous proof shows how to calculate  $\gamma_0$ , and we will illustrate this for two well known population models, namely Hassell [22] and Ricker [11] models. The per-capita production function of the former is  $g(x) = \lambda(1 + a x)^{-b}$ , where  $\lambda > 0$  represents the intrinsic rate of population growth,  $b > 0$  determines the strength of density dependence, and  $a > 0$  is a scaling parameter. This model satisfies conditions (i), (ii) and (iv) for  $\lambda > 1$  and  $b > 1$ . In the absence of harvesting, the positive equilibrium  $K = (\lambda^{\frac{1}{b}} - 1)/a$  is unstable for  $b > 2$  and  $\lambda > (b/(b - 2))^b$ . In this model,  $d = 1/(a(b - 1))$  and  $\gamma_0$  is either null or the unique solution of

$$\lambda = \frac{1}{1 - \gamma} \left( \frac{b - \gamma}{b - 1} \right)^b. \tag{6}$$

For fixed  $b$ , the function  $k(\gamma)$  given by the right-hand side of (6) is strictly increasing and satisfies  $k \rightarrow (b/(b - 1))^b$  for  $\gamma \rightarrow 0$  and  $k \rightarrow +\infty$  for  $\gamma \rightarrow 1$ . Hence, for  $\lambda > (b/(b - 1))^b$  the value  $\gamma_0 > 0$  is implicitly given by  $k(\gamma_0) = \lambda$ , and  $\gamma_0 = 0$  otherwise. For  $\lambda = 7.7$  and  $b = 50$ , we obtain  $\gamma_0 \approx 0.848$  and  $\gamma^* \approx 0.870$ . Thus, for any  $\gamma \in [0.848, 0.870]$  the positive

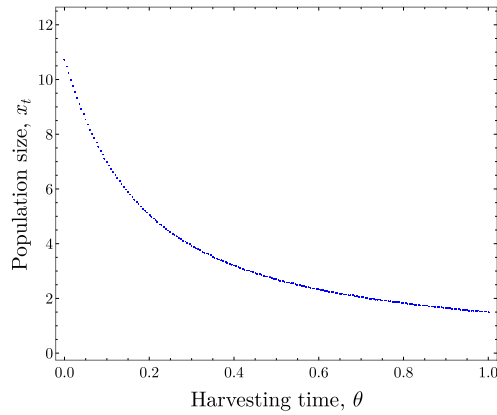


**Fig. 2.** Bifurcation diagram of population model (4) for varying harvesting times  $\theta \in [0, 1]$ . The underlying population dynamics is given by the Hassell map  $g(x) = 7.7(1 + 10^{-3} \cdot x)^{-50}$ , and the harvesting effort is  $\gamma = 0.86$ .

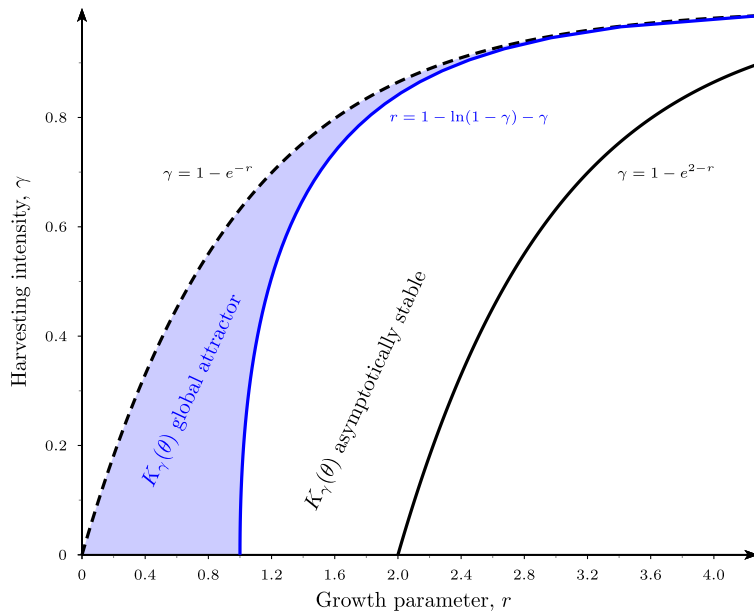


**Fig. 3.** Parameters inside the region between the black curves guarantee that  $K_\gamma(\theta)$  is asymptotically stable for all  $\theta \in [0, 1]$  for (4) in the Ricker case. The blue area specifies the region in the  $(r, \gamma)$ -parameter space for which Proposition 2 guarantees the global attraction of the positive equilibrium. (For interpretation of the references to color in this figure legend, the reader is referred to the web version of this article).

equilibrium  $K_\gamma(\theta)$  is stabilized by the effect of harvesting and acts as a global attractor for all  $\theta \in [0, 1]$ . This can be appreciated in Fig. 2.

In the case of Ricker model, the per-capita production function is  $g(x) = e^{r(1-x)}$ , where  $r > 0$  is a growth parameter. In this case, conditions (i), (ii) and (iv) are met for all  $r > 0$ . Proposition 3.4 in [1] guarantees for this model that the positive equilibrium  $K_\gamma(\theta)$  of (4) with  $\theta \in [0, 1]$  is asymptotically stable if  $1 - e^{2-r} < \gamma < 1 - e^{-r}$ . The curves defined by these inequalities delimit a region in the  $(r, \gamma)$ -parameter space shown in Fig. 3. Proposition 2 provides a subregion for which the positive equilibrium is indeed a global attractor. In this case,  $d = \frac{1}{r}$  and  $\gamma_0$  is either zero or the unique solution of

$$r = 1 - \ln(1 - \gamma) - \gamma. \tag{7}$$

The function  $h(\gamma) = 1 - \ln(1 - \gamma) - \gamma$  is strictly increasing and verifies  $h \rightarrow 1$  for  $\gamma \rightarrow 0$  and  $h \rightarrow +\infty$  for  $\gamma \rightarrow 1$ . Hence, for  $r > 1$  the value  $\gamma_0 > 0$  is implicitly given by  $h(\gamma_0) = r$ , and for  $r \in (0, 1]$ ,  $\gamma_0 = 0$ . The blue region in Fig. 3 corresponds to the subregion in the  $(r, \gamma)$ -parameter space defined by this curve.

### 4. Stability in the Ricker case

#### 4.1. Global stability for any harvesting time

**Proposition 2** gives a sufficient condition for the global stability of the positive equilibrium for (4) in the Ricker case. But as the growth parameter  $r$  increases, the harvesting intensity has to be chosen higher and very close to  $\gamma^* = 1 - e^{-r}$ ; see Fig. 3. This has two important drawbacks commented in the introduction: it could be considered dangerous and it may be difficult to attain in real situations.

In this section, we present a global stability result for (4) in the Ricker case valid for harvesting efforts below  $\gamma = \rho_0 \approx 0.635$ . The proof is based on a global stability result for S-maps.

**Definition 1.** The map  $h: (0, \infty) \rightarrow (0, \infty)$  is a S-map if:

- (S1)  $h$  is a  $C^3$  map and  $h'$  vanishes at most at one point  $d$  (which is a relative extremum of  $h$ );
- (S2) there is  $K \in (0, \infty)$  such that  $h(x) > x$  (respectively,  $h(x) < x$ ) for any  $x < K$  (respectively,  $x > K$ );
- (S3)  $Sh(x) < 0$  for any  $x \in (0, \infty)$  (except possibly at  $d$ ), where

$$Sh(x) := \frac{h'''(x)}{h'(x)} - \frac{3}{2} \left( \frac{h''(x)}{h'(x)} \right)^2$$

is the Schwarzian derivative of  $h$ .

For S-maps the following property can be derived from results in [16,23]. We recommend to read the introduction of [24] for more details and a nice discussion of the role of the negative Schwarzian derivative in discrete dynamical systems.

**Lemma 1** (Allwright–Singer). *If  $h$  is a S-map and  $|h'(K)| \leq 1$ , then  $K$  is a global attractor of  $x_{n+1} = h(x_n)$ .*

**Proposition 1** implies that  $F_\theta$  satisfies (S2) for all  $\theta \in [0, 1]$  if  $\gamma < \gamma^*$ . On the other hand, maps  $F_0$  and  $F_1$  are S-maps [10]. But this is not enough to guarantee that the convex combination  $F_\theta$  is a S-map. Thus, in order to apply Lemma 1, we need sufficient conditions guaranteeing that  $F_\theta$  satisfies conditions (S1) and (S3) for all  $\theta \in [0, 1]$ . We begin with (S1).

**Lemma 2.** *Assume  $g(x) = e^{r(1-x)}$  and  $r > 0$ . If  $\gamma \in (0, 2/3)$ , then  $F_\theta$  satisfies (S1).*

**Proof.** Differentiating, we have

$$F'_1(x) = (1 - \gamma)[1 - rx]e^{r(1-x)},$$

so  $F_1$  has only one critical point  $C_\gamma(1) = 1/r$ , which is a strict positive maximum. Similarly,  $F_0$  has only one critical point  $C_\gamma(0) = \frac{1}{(1-\gamma)r}$ , which is a strict maximum as well. Since the graph of  $F'_\theta$  is between the graphs of  $F'_1$  and  $F'_0$ , then  $F'_\theta$  is strictly positive before  $C_\gamma(1)$  and strictly negative after  $C_\gamma(0)$ . In consequence, all the critical points of  $F_\theta$  lie in  $[C_\gamma(1), C_\gamma(0)]$  and at least one of them is a relative maximum.

We want to show that fixing  $\gamma \in (0, \frac{2}{3})$  impedes the existence of more than one critical point in  $[C_\gamma(1), C_\gamma(0)]$ . Note that if  $F'_\theta$  intersects the horizontal axis more than once in  $[C_\gamma(1), C_\gamma(0)]$ , then, by Rolle’s Theorem,  $F''_\theta$  has two different zeros in  $[C_\gamma(1), C_\gamma(0)]$ . But this is impossible because  $\gamma \in (0, \frac{2}{3})$  guarantees that  $F''_\theta$  is strictly increasing on  $[C_\gamma(1), C_\gamma(0)] \subset (0, \frac{3}{r})$ . Indeed, differentiating

$$F''_1(x) = (1 - \gamma)r^2(3 - rx)e^{r(1-x)},$$

and

$$F''_0(x) = (1 - \gamma)^3r^2[(3 - (1 - \gamma)rx)]e^{r(1-(1-\gamma)x)}.$$

Thus, recalling that  $F''_\theta$  is the convex combination of  $F''_0$  and  $F''_1$ ,  $F''_\theta$  is strictly increasing on  $(0, \frac{3}{r})$ . Finally, since  $\gamma < \frac{2}{3}$ , we have

$$C_\gamma(0) = \frac{1}{r(1-\gamma)} < \frac{3}{r}$$

and  $[C_\gamma(1), C_\gamma(0)] \subset (0, \frac{3}{r})$ . □

As for condition (S3), we will completely characterize, in terms of  $\gamma$ , when  $F_\theta$  has a negative Schwarzian derivative for all  $\theta \in [0, 1]$ .

Let  $\rho_0 \in \mathbb{R}$  be the smallest positive root of the 6th degree polynomial

$$Q(\gamma) = 2\gamma^6 + 36\gamma^5 + 99\gamma^4 - 162\gamma^3 - 189\gamma^2 + 324\gamma - 108.$$

We can prove by bisection that  $Q(\gamma)$  has six distinct real roots and that

$$0.63524635 < \rho_0 < 0.63524637.$$

**Lemma 3.** *Assume  $g(x) = e^{r(1-x)}$  and  $r > 0$ . Then  $SF_\theta(x) < 0$  for all  $\theta \in [0, 1]$  and  $x \geq 0$  if and only if  $\gamma < \rho_0$ .*

**Proof.** For  $x \in (0, \infty)$  and  $\gamma \in (0, 1)$ , define

$$\begin{aligned} \mathbf{u}_0 &= (F'_0(x), F''_0(x), F'''_0(x)), \\ \mathbf{u}_1 &= (F'_1(x), F''_1(x), F'''_1(x)). \end{aligned}$$

As the Schwarzian derivative of  $F_\theta$  at  $x$  is

$$SF_\theta(x) = \frac{2F'''_\theta(x)F'_\theta(x) - 3F''^2_\theta(x)}{2F_\theta'^2(x)},$$

we consider the bilinear form  $N : \mathbb{R}^3 \times \mathbb{R}^3 \rightarrow \mathbb{R}$  defined by

$$N(\mathbf{v}, \mathbf{w}) = v_1w_3 + w_1v_3 - 3v_2w_2,$$

the associated quadratic form of which is  $N(\mathbf{v}, \mathbf{v}) = 2v_1v_3 - 3v_2^2$ .

The necessary and sufficient condition for the Schwarzian derivative  $SF_\theta(x)$  to be negative for all  $\theta$  is that  $N(\mathbf{u}_0, \mathbf{u}_1) < \sqrt{N(\mathbf{u}_0, \mathbf{u}_0)N(\mathbf{u}_1, \mathbf{u}_1)}$  (see Lemma 4 in the Appendix).

Next, we write  $z = xr$ . For a fixed  $\gamma \in (0, 1)$ , consider the following quartic polynomial (see the Appendix for the calculations):

$$\begin{aligned} P(z) &:= \frac{N(\mathbf{u}_0, \mathbf{u}_0)N(\mathbf{u}_1, \mathbf{u}_1) - (N(\mathbf{u}_0, \mathbf{u}_1))^2}{[r^2 e^{2r-2z+z\gamma} (\gamma - 1)^2 \gamma]^2} \\ &= a_4z^4 + a_3z^3 + a_2z^2 + a_1z + a_0, \end{aligned} \tag{8}$$

where

$$\begin{aligned} a_4 &= (\gamma - 1)^2(-\gamma^2 - 2\gamma + 2), \\ a_3 &= 2(2 - \gamma)(1 - \gamma)(\gamma^2 + 3\gamma - 3), \\ a_2 &= -\gamma^4 + 6\gamma^3 + 30\gamma^2 - 72\gamma + 36, \\ a_1 &= 6(2 - \gamma)(\gamma^2 + 4\gamma - 4), \\ a_0 &= -9(\gamma^2 + 4\gamma - 4). \end{aligned} \tag{9}$$

The discriminant of  $P(z)$  is (see, for example, [25, Theorem 6.8] for the formula of the discriminant of a quartic polynomial):

$$\Delta(\gamma) = 432(\gamma^2 + 4\gamma - 4)^3(\gamma - 1)^6Q(\gamma).$$

All roots of  $\Delta$

$$\rho_{-4} < \dots < \rho_0 < \dots < \rho_4$$

are real and two of these roots correspond to the values of  $\gamma$  for which zero is a root of  $P(z)$ .

The coefficients of  $P(z)$  depend continuously on  $\gamma$ , and the roots of the discriminant correspond to the values of  $\gamma$  for which real roots are created and destroyed. Therefore, by selecting one particular value of  $\gamma$  in each of the intervals  $(0, \rho_0)$ ,  $(\rho_0, \rho_1)$ ,  $\dots$ ,  $(\rho_3, \rho_4)$  and calculating the roots of these five concrete quartic polynomials, we obtain that only for  $\gamma \in (0, \rho_0)$  the polynomial  $P(z)$  has no positive roots.

We conclude that  $SF_\theta$  is negative for all  $\theta \in [0, 1]$  and  $x > 0$  if only if  $\gamma \in (0, \rho_0)$ .  $\square$

**Theorem 1.** Assume  $g(x) = e^{r(1-x)}$ ,  $r > 0$  and  $\gamma < \rho_0$ . If the positive equilibrium  $K_\gamma(0)$  of (4) with  $\theta = 0$  is asymptotically stable and

$$\gamma \in [1 - e^{2-r}, 1 - e^{-r}]. \tag{10}$$

holds, then the fixed point  $K_\gamma(\theta)$  is asymptotically stable for (4) for all  $\theta \in [0, 1]$  and all positive solutions of (4) converge to  $K_\gamma(\theta)$ .

**Proof.** The asymptotic stability was proved in [1, Proposition 3.4]. Since we know by Lemma 2 that  $F_\theta$  satisfies (S1), by Proposition 1 that (S2) holds, and by Lemma 3 that  $SF_\theta < 0$ , the result follows as a direct application of Lemma 1.  $\square$

Fig. 4 illustrates the improvement of adding the region of parameters  $(r, \gamma)$  for which changing timing does not affect the global attraction of the positive equilibrium given by Theorem 1 to that previously given by Proposition 2 (see Fig. 3 for comparison).

To discuss the relevance of Theorem 1 in the context of applicability, let us suppose that we want to implement a proportional harvesting control that globally stabilizes the system for  $r = 2.7$  around  $x^* = 1$ . Lemma 2.3 in [26] guarantees that this can be achieved by fixing the harvesting effort at a value  $1 - \Phi(f^{-1}(1)) \approx 0.9156$ , where  $\Phi(x) = 1/g(x)$  and  $f(x) = xg(x)$ . Implementing this control in real populations can be problematic for two main reasons. On the one hand, the removal intensity is close to the persistence limit  $\gamma^* \approx 0.9328$ , thus implying a serious risk of extinction. On the other hand, removing such a high proportion of individuals may be difficult or impossible to attain in many practical situations. Theorem 1 yields an alternative without these drawbacks, since it guarantees that for any  $\gamma \in [1 - e^{2-r}, \rho_0] \approx [0.5034, 0.6352]$  the positive

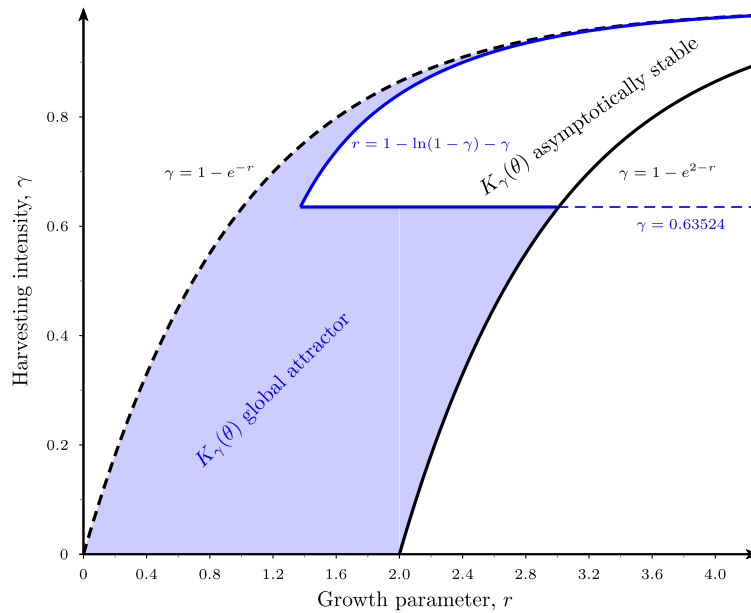


**Fig. 4.** The blue area is the region in the  $(r, \gamma)$ -parameter space for which changing timing does not affect the global attraction of the positive equilibrium of model (4) in the Ricker case (Theorem 1 and Proposition 2). (For interpretation of the references to color in this figure legend, the reader is referred to the web version of this article).

equilibrium  $K_{\gamma}(\theta)$  acts as a global attractor. Suppose we fix  $\gamma = 0.55$ . For this value,  $K_{0.55}(0) \approx 1.5650$  and  $K_{0.55}(1) \approx 0.7043$ . According to Proposition 3.2 in [1],  $K_{0.55}(\theta)$  is a decreasing function of  $\theta$  that continuously covers the range between  $K_{0.55}(0)$  and  $K_{0.55}(1)$ . Thus, it is possible to find a moment for the intervention such that  $K_{0.55}(\theta) = 1$ ; in this case  $\theta \approx 0.6421$ . In conclusion, Theorem 1 provides an alternative way to attain the desired stabilizing effect with a significantly lower effort by conveniently delaying the intervention.

4.2. Stability depending on timing

Our last result for the Ricker case explores under which conditions timing can be stabilizing by itself. We prove that it is possible to find  $\theta \in (0, 1)$  such that  $K_{\gamma}(\theta)$  for (4) is stable when  $K_{\gamma}(0)$  is unstable.

**Proposition 3.** Assume  $g(x) = e^{r(1-x)}$  and  $r > 0$ . Then, there exist  $\gamma_c < \gamma_* := 1 - e^{-2}$  such that for any  $\gamma \in (\gamma_c, \gamma_*)$  it is possible to find a timing interval  $(\theta_0, \theta_1)$  with the property that for each  $\theta \in (\theta_0, \theta_1)$  the fixed point  $K_{\gamma}(\theta)$  is asymptotically stable for (4).

**Proof.** Differentiating, we obtain  $F_1'(x) = (1 - \gamma)r(2 - rx)e^{r(1-x)}$ , and thus  $F_1'$  is strictly decreasing to the left of  $2/r$  and strictly increasing to the right. On the other hand, it is easy to check that for  $\gamma = \gamma_*$  the fixed point of  $F_1$  coincides with the above inflection point (i.e.,  $K_{\gamma_*}(1) = 2/r$ ), and  $F_1'(K_{\gamma_*}(1)) = -1$ . In that case,  $F_1'(x) \geq -1$  for all  $x$ .

The equalities

$$\begin{aligned} F_0(x) &= F_1((1 - \gamma)x)/(1 - \gamma), \\ F_0'(x) &= F_1'((1 - \gamma)x), \\ F_0''(x) &= (1 - \gamma)F_1''((1 - \gamma)x), \end{aligned}$$

yield similar conclusions regarding  $F_0$ : the unique inflection point (equal to  $2/(r(1 - \gamma))$ ) coincides with the fixed point  $K_{\gamma_*}(0)$ , and moreover  $F_0'(K_{\gamma_*}(0)) = -1$ .

For  $\gamma < \gamma_*$ , the fixed points  $K_{\gamma}(0)$  and  $K_{\gamma}(1)$  are unstable (see Proposition 3.3 in [1]) and the sets  $(F_0')^{-1}(-1)$  and  $(F_1')^{-1}(-1)$  contain two points (in addition to the mentioned monotonicity properties for  $F_1'$ , note that  $F_1'(0^+) = (1 - \gamma)e^r$  and  $F_1'(x) \rightarrow 0$  as  $x \rightarrow \infty$ ). Let denote  $a = \max\{(F_1')^{-1}(-1)\}$  and  $b = \min\{(F_0')^{-1}(-1)\}$ . It is immediate that  $a > K_{\gamma}(1)$  and  $b < K_{\gamma}(0)$  because  $F_0'(K_{\gamma}(0))$  and  $F_1'(K_{\gamma}(1))$  are less than  $-1$ . By continuity, for  $\gamma \uparrow \gamma_*$  we have

$$\max\left\{K_{\gamma}(1), \frac{2}{r}\right\} < a < b < \min\left\{K_{\gamma}(0), \frac{2}{r(1 - \gamma)}\right\}. \tag{11}$$

The inflection point of  $F_1$  does not depend on  $\gamma$ , whereas the one of  $F_0$  decreases as  $\gamma$  increases. For  $\gamma \rightarrow 0$  both points coincide and hence, by continuity, there must exist some  $\gamma < \gamma_*$  for which  $a = b$ . Let  $\gamma_c$  be the maximal value of  $\gamma$  satisfying this last condition. It is immediate that (11) is met for all  $\gamma \in (\gamma_c, \gamma_*)$ . Since  $F_1'$  is strictly increasing to the right

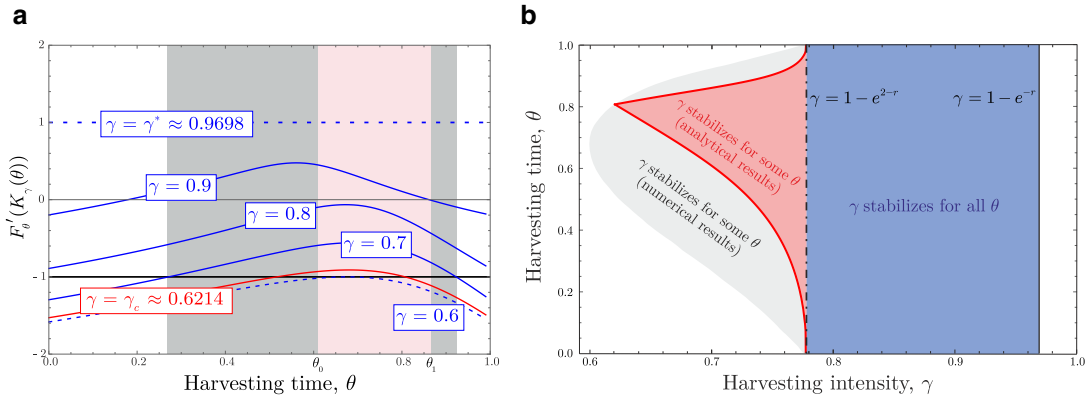


**Fig. 5.** Panel (A): stability of the positive equilibrium of (4) in terms of the harvesting time  $\theta \in [0, 1]$  for different values of the removal intensity  $\gamma$ . The positive equilibrium  $K_\gamma(\theta)$  is stable if  $-1 < F'_\theta(K_\gamma(\theta)) < 1$ . The gray area corresponds to the actual range of stabilizing harvest times for  $\gamma = 0.7$ , and the red area to the range  $[\theta_0, \theta_1]$  derived from Proposition 3. Panel (B): the gray region shows numerical results for the combinations of  $\gamma$  and  $\theta$  for which  $K_\gamma(0)$  is unstable and  $K_\gamma(\theta)$  is asymptotically stable. The red region corresponds to values guaranteed to be stabilizing (by Proposition 3). In both panels, the underlying population dynamics is given by the Ricker map  $g(x) = e^{3.5(1-x)}$ . (For interpretation of the references to color in this figure legend, the reader is referred to the web version of this article).

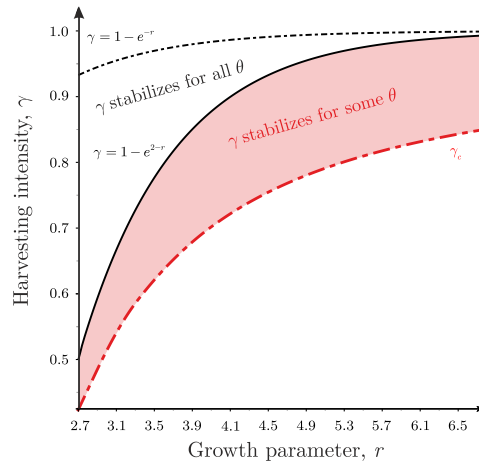


**Fig. 6.** The red region corresponds to harvesting intensities  $\gamma$  that are destabilizing for a given growth parameter  $r$  when individuals are removed at the beginning or at the end of the reproductive season and for which there exists a stabilizing harvesting time  $\theta$  according to Proposition 3. (For interpretation of the references to color in this figure legend, the reader is referred to the web version of this article).

of  $2/r$  and  $F'_0$  is strictly decreasing to the left of  $2/(r(1-\gamma))$ , we conclude that  $F'_1(x) > -1$  and  $F'_0(x) > -1$  for all  $x \in (a, b)$ . This leads to  $F'_\theta(x) > -1$  because  $F'_\theta$  is a convex combination of  $F'_0$  and  $F'_1$ .

The fixed point  $K_\gamma(\theta)$  strictly decreases and continuously covers the interval  $[K_\gamma(1), K_\gamma(0)] \supset (a, b)$  for varying  $\theta$ . Hence, there must exist  $\theta_0, \theta_1 \in (0, 1)$  such that  $K_\gamma(\theta_0) = b$  and  $K_\gamma(\theta_1) = a$ . In particular,  $K_\gamma(\theta) \in (a, b)$  for all  $\theta \in (\theta_0, \theta_1)$ , and thus  $F'_\theta(K_\gamma(\theta)) > -1$ .  $\square$

For fixed values of the growth parameter  $r$ , the proof of Proposition 3 yields a method for determining a range of removal intensities  $\gamma$  for which there exist harvest moments  $\theta$  that stabilize the positive equilibrium  $K_\gamma(\theta)$ . Moreover, for a fixed  $\gamma$  it also provides a method for determining a range of stabilizing times  $\theta_0 \leq \theta \leq \theta_1$ . We illustrate this for the growth parameter  $r = 3.5$ , for which the limit of population persistence is  $\gamma^* = 1 - e^{-3.5} \approx 0.9698$ . Numerical simulations reveal that  $\gamma_c \approx 0.6214$ , and thus Proposition 3 guarantees the existence of stabilizing harvest times for all  $\gamma \in [0.6214, 0.9698]$ . Fig. 5(A) shows that this range is quite accurate: there are no stabilizing times for harvesting efforts slightly below  $\gamma_c$ . Consider the control intensity  $\gamma = 0.7 \in [\gamma_c, \gamma^*)$ . It can be numerically found that  $\theta_0 \approx 0.6086$  and  $\theta_1 \approx 0.8611$ . The blue area in Fig. 5(A) corresponds to this range, and the red area represents the actual range of times that stabilize  $K_\gamma(\theta)$ . Compared to the range of harvesting efforts, the range of stabilizing intervention moments given by Proposition 3 seems to be more conservative. However, this range is wide enough to allow for the determination of stabilizing harvest times with reasonable certainty. Fig. 5(B) shows the actual range of these times and the range defined by Proposition 3 in terms of the removal intensity  $\gamma$ .

Finally, we emphasize that Proposition 3 implies that harvest timing can be very useful from a practical point of view since it can be used to significantly enlarge the range of harvesting efforts that are able to stabilize the population for a fixed  $r$  (see Fig. 6).

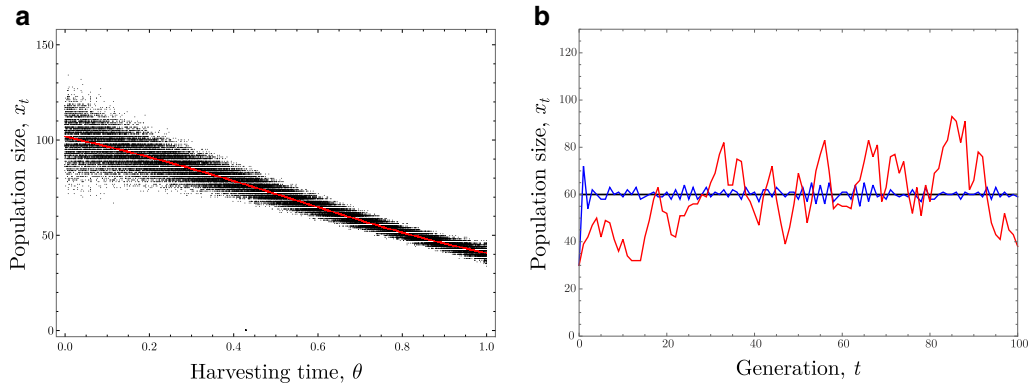


**Fig. 7.** Panel (A): bifurcation diagram of (4) (red dots) and (12) (black dots) with  $\gamma = 0.6$  and  $\sigma = 0.015$  for varying harvesting time  $\theta \in [0, 1]$ . The underlying population dynamics is given by the Ricker map  $g(x) = e^{2.85(1-x/60)}$ . Panel (B): the red curve gives the size of a population governed by (12) with  $\gamma = 0.9292$  and  $\theta = 0$ , and the blue curve for  $\gamma = 0.6$  and  $\theta = 0.6688$ . In both cases, the initial population size is  $x_0 = 30$  and the level of noise is  $\sigma = 0.015$ . (For interpretation of the references to color in this figure legend, the reader is referred to the web version of this article).

### 4.3. Introducing biological realities

So far, we have analyzed how changing harvest times can affect the stability of populations described by theoretical deterministic equations. In this section, we check the robustness of our results on more realistic models. To this end, we consider the parameter estimates obtained in [27] on the basis of time series data for laboratory populations of the fruit fly *Drosophila melanogaster*. The per-capita production function is  $g(x) = e^{r(1-x/K)}$ , which corresponds to the non-scaled Ricker model with carrying capacity  $K$  and growth parameter  $r$ . For the different populations, the estimated growth parameter ranged from 2.7 to 3.0 (see [27], Supplementary material). We fix  $r$  in the midpoint of this range, i.e.,  $r = 2.85$ , and the carrying capacity at  $K = 60$ .

We extend the above model by introducing two biological realities. The first of them follows from the fact that individuals always come and are harvested in whole numbers. It is well established that the dynamics of a discrete-state system can be quite different from its continuous-state version, a phenomenon known as lattice effect [28]. Consequently, we integerize population sizes to make the model more realistic. The second extension to be considered is stochasticity. This is clearly more problematic, since stabilizing an equilibrium under the effect of noise is not possible unless the magnitude of the noise tends to zero as time grows. We follow the work of Braverman et al. [29] to generalize the notion of global stability to stochastic systems: equilibria of stochastic difference equations (blurred equilibrium) are points for which all trajectories eventually enter some interval around them. Since stochasticity is in many cases involved in the control, we propose a integerized stochastic version of (4) based on introducing noise in the removal intensity in the form

$$x_{t+1} = \text{int}([\theta g(x_t) + (1 - \theta)g((1 - \gamma + \sigma v_{t+1})x_t)](1 - \gamma + \sigma v_{t+1})x_t), \tag{12}$$

where  $\sigma$  is a parameter measuring the level of noise and  $(v_t)_{t \in \mathbb{N}}$  is a sequence of independent random variables uniformly distributed in  $[-1, 1]$ , whereas function  $\text{int}(x)$  gives the integer closest to  $x$  (if  $x + 0.5 \in \mathbb{N}$ , then  $\text{int}(x)$  gives the even integer closest to  $x$ ).

According to Theorem 1, the positive equilibrium of (4) for any intervention time  $\theta$  is a global attractor for harvesting efforts  $\gamma \in [1 - e^{-2.85}, \rho_0] \approx [0.5726, 0.6352]$ . Fig. 7(A) shows that the same point is a blurred equilibrium of (12). We conclude therefore that the stabilization of populations induced by harvesting at intermediate moments during the reproductive season is robust under the effect of both noise and lattice effect. Interestingly, we observe that timing helps to damp the destabilizing effect of noise: the range of fluctuation of the population size can be significantly reduced if the intervention is conveniently delayed.

We can go further and analyze how timing can be helpful to stabilize the population size in the presence of noise around a specific value, for instance  $x^* = 60$ . Theorem 3.5 in [26] guarantees that if harvesting is implemented at the beginning of the reproductive season ( $\theta = 0$ ) with an intensity  $\gamma(x^*) \approx 0.9292$ , the size of the population governed by the non-integerized version of (12) is stabilized around  $x^* = 60$  with a fluctuation range that depends on the level of noise. As per Theorem 1, numerical simulations reveal that for  $\gamma = 0.6$  and  $\theta = 0.6688$  the point  $x^* = 60$  is a global attractor of the deterministic system (4). Fig. 7(B) shows that the population governed by the integerized stochastic Eq. (12) is also stabilized around this point. This confirms again that the stabilizing properties of timing are not affected by neither stochasticity nor lattice effect. Moreover, we observe that stabilizing the population with delayed intervention has several advantages. Firstly, the proportion of individuals to be removed in each generation is significantly lower. This is expected to allow for the stabilization of populations that would be impossible to control due to practical limitations in case of being harvested at the beginning of the reproductive period. Secondly, the intensity of the intervention places the population far from the extinction risk associated with harvesting efforts above the persistence limit  $\gamma^* \approx 0.9421$ . Finally, when individuals are removed at an intermediate moment during the reproductive season, the fluctuation in the population size is lower than if

they were harvested at the beginning of this period. This last fact can be evaluated in terms of the fluctuation index (FI), which was introduced in [27] as a dimensionless measure of the average one-step variation of the population size scaled by the average population size in a certain period. For a time period of  $T$  steps, it is given by

$$FI = \frac{1}{T\bar{x}} \sum_{t=0}^{T-1} |x_{t+1} - x_t|,$$

where  $\bar{x}$  is the mean population size of the  $T$  generations. We have averaged the FI over 500 time series of length 1000 with initial conditions chosen as pseudo-random numbers in  $(0, dg(d)]$ , ignoring the first 100 steps. If individuals are harvested with an intensity  $\gamma = 0.9292$  at the beginning of the season, the FI is 0.111. If the intervention takes place at a time  $\theta = 0.6688$  during the season with an intensity  $\gamma = 0.6$ , the FI decreases to 0.050. This is consistent with what was observed in Fig. 7(A): a delay in the intervention can reduce the fluctuations in size around the equilibrium.

**5. Timing can be destabilizing**

In the previous section, we have seen that timing can be stabilizing by itself. In view of this, it is logical to ask the opposite question: *can timing be destabilizing?* Based on both numerical simulations and analytical results, Cid et al. conjectured in [1] that harvesting times  $\theta$  in the interior of  $[0, 1]$  cannot be destabilizing if conditions (i), (ii) and (iv) are satisfied.

**Conjecture 1** (Conjecture 3.5, [1]). *Assume that conditions (i), (ii) and (iv) hold. If the positive equilibrium  $K_\gamma(0)$  of (4) with  $\theta = 0$  is asymptotically stable, then the fixed point  $K_\gamma(\theta)$  is asymptotically stable for (4) for all  $\theta \in [0, 1]$ .*

Suppose that  $K_\gamma(0)$  is asymptotically stable. If Conjecture 1 was true, then we could delay the time of intervention  $\theta \in [0, 1]$  without affecting the stability of the positive equilibrium  $K_\gamma(\theta)$ . This freedom to choose the time of intervention is clearly desirable from a management point of view. However, the conjecture is false. We provide a counterexample. To build it, we use the map  $h: [0, 1] \rightarrow [0, 1]$  defined by

$$h(x) = x \left( \frac{786}{100} - \frac{2331}{100}x + \frac{2875}{100}x^2 - \frac{133}{10}x^3 \right).$$

This map was introduced in [16] as an example of unimodal map with negative Schwarzian derivative having two attractors. Now, we define  $g: [0, \infty) \rightarrow [0, \infty)$  by

$$g(x) = \begin{cases} 2 \frac{h(x)}{x}, & x \in [0, \frac{9}{10}), \\ \frac{591}{625} e^{-\frac{57397}{7500}(x-\frac{9}{10})}, & x \in (\frac{9}{10}, \infty). \end{cases} \tag{13}$$

We note that at the splice point  $9/10$  the function  $g$  is differentiable.

It is not hard to see that the map  $g$  satisfies conditions (i), (ii) and (iv), see Fig. 8(A). Moreover, system (1) has an unstable positive equilibrium, see Fig. 8(A).

Next, we fix  $\gamma = 0.565$ . Fig. 8(B) shows that this harvesting effort applied at the beginning or at the end of the reproductive season stabilizes a fixed point. Thus, the positive equilibrium  $K_\gamma(0)$  is asymptotically stable for  $\theta = 0$ . However, for  $\theta = 0.7$  the convex combination of  $F_1$  and  $F_0$  crosses the diagonal with slope greater than 1 in absolute value (see Fig. 8(B)). Thus, the positive equilibrium is unstable for  $F_{0.7}$ . The explanation for this effect is as follows, for this map the intensity of the overcompensation abruptly increases for certain interval of population sizes. This makes the graph of  $xg(x)$  to have a steep negative slope in that interval and such a slope is inherited by the graph of  $F_1$ , although attenuated by a  $(1 - \gamma)$  factor. Since  $F'_\theta$  is the convex combination of  $F'_1$  and  $F'_0$ , when the positive equilibrium  $K_\gamma(\theta)$  is in the interval where  $F'_1 \ll -1$  we can have that  $F'_\theta < -1$ .

Actually, a bifurcation diagram taking  $\theta$  as the bifurcation parameter shows that delaying the harvesting time  $\theta$  leads to the emergence of bubbles (see [30, Definition 3]). This is illustrated in Fig. 9. We point out that bubbles for (4) were studied in [1], but with a different approach. There it was numerically shown for the Clark-Ricker bimodal map that bubbles related to a variation in the harvesting effort for  $\theta = 0$  disappear when harvesting occurs at an intermediate moment of the season, thereby demonstrating that intermediate harvesting times can have a stabilizing effect. Here, however, the bubble is related to a variation in the harvesting time  $\theta$  for a unimodal map and implies that intermediate harvesting times can have a destabilizing effect.

**Remark 1.** The counterexample of Conjecture 1 given by (13) corresponds to a piecewise function obtained by extending the function  $\frac{2h(x)}{x}$  to  $[0, +\infty)$ . We highlight that this fact has no influence on the result: the tail of the per-capita production function does not affect the stability of the positive equilibrium. On the other hand, the counterexample to Conjecture 1 is by non means unique. Indeed, for the analytic function

$$g(x) = e^{6-15x+15x^2-\frac{11}{2}x^3}, \tag{14}$$

we have that  $\frac{dF_{0.6}}{dx}(K_{0.5}(0.6)) = F'_{0.6}(K_{0.5}(0.6)) \approx -1.27786$  while  $F'_0(K_{0.5}(0)) = F'_1(K_{0.5}(1)) \approx -0.206984$ , and so this function provides another counterexample to Conjecture 1.

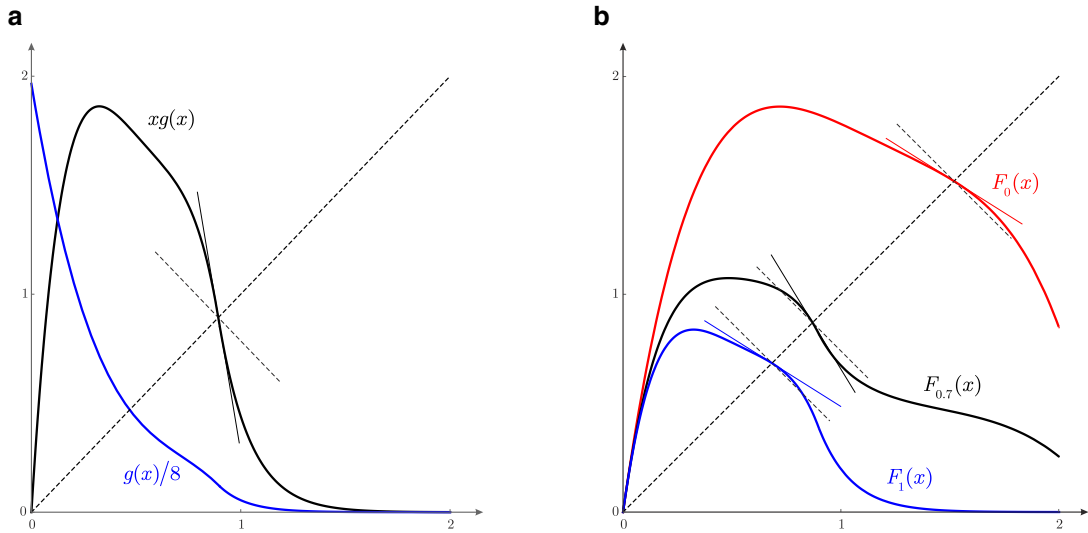


**Fig. 8.** Panel (A): the blue curve corresponds to the graph of  $g(x)$ , which was vertically compressed by a factor  $1/8$  to improve the representation; the black curve corresponds to the graph of  $xg(x)$ , showing that this map satisfies (iv) and has an unstable positive fixed point. Panel (B): harvesting effort fixed to  $\gamma = 0.55$ . The blue, red and black curves correspond to the graphs of  $F_1(x)$ ,  $F_0(x)$  and  $F_{0.7}(x)$ , respectively; observe that  $K_{0.5}(0)$  is asymptotically stable whereas  $K_{0.5}(0.7)$  is unstable. (For interpretation of the references to color in this figure legend, the reader is referred to the web version of this article).

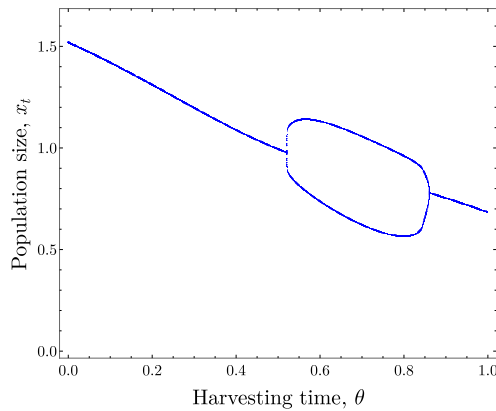


**Fig. 9.** Bifurcation diagram of the population model (4) for varying harvesting time  $\theta \in [0, 1]$ . The harvest effort is fixed to 0.55, and the underlying population dynamics is described by (13). The positive equilibrium is asymptotically stable for  $\theta = 0$  and  $\theta = 1$ , but for an interval of values of  $\theta \in (0, 1)$  this positive equilibrium is unstable because of the presence of a bubble.

**6. Discussion and conclusions**

In this paper, we have studied the combined effect of harvesting intensity and harvesting time on the stability of a discrete population model proposed by Seno [7]. Despite the fact that this model is one of the simplest models to account for variable harvest timings, it is suitable to gain some basic understanding of how the timing of interventions affects the stability of controlled populations.

Under general conditions, we have shown in Proposition 2 that timing has no negative effect on the stability of the positive equilibrium if the harvesting intensity is close enough to  $\gamma^*$  (see Fig. 3). Moreover, we have shown that the latter stability is global. To the best of our knowledge, this is the first global stability result for (4) valid for general overcompensatory population models, since global stability results in [1] only cover undercompensatory models (such as the Beverton–Holt model [31]) and the quadratic model.

From a practical point of view, global stability is always desirable since it allows to predict the long term behavior independently of the initial condition. Nevertheless, high intensities close to  $\gamma^*$  may be considered undesirable and unrealistic from an environmental management point of view. First, because  $\gamma^*$  is an extinction threshold for the species, harvesting intensities above  $\gamma^*$  cause the extinction of the population. Second, because high harvesting intensities are expected to be more labour intensive and have high operating costs.

In the Ricker–Seno model, we have investigated whether for low or medium harvesting intensities there is global stability of the positive equilibrium regardless of the time of the intervention. **Theorem 1** provides a sufficient condition based on a classical global stability result for S-maps [16,23].

Additionally, we have rigorously shown for the Ricker–Seno model that timing can be stabilizing, that is, a harvesting intensity applied at an appropriate time of the season can asymptotically stabilize the positive equilibrium even when it cannot be stabilized at the beginning or the end of the reproductive season with the same harvesting intensity.

Due to its simplicity, Seno’s model has some important limitations that must be taken into account. First, a constant duration of the period in which individuals accumulate energy for reproduction is implicitly assumed. This may be unrealistic in practical applications since it is well established that environmental conditions affect the length of the reproductive season of some species of birds and mammals [32–34]. Second, the model fixes for all generations a harvesting moment  $\theta$  during the season that can be arbitrarily chosen. Due to practical limitations, this freedom of choice may be impossible in certain situations. For instance, this would be the case of salmon, which keep concentrated during reproduction and disperse afterwards. Third, the model is deterministic and assumes a continuum of system states. Numerical simulations indicate that timing enhances the stabilizing properties of harvesting in the presence of both noise and lattice effect.

Finally, we have shown that timing can be destabilizing under natural conditions assumed on population production maps. This provides counterexamples for a conjecture recently published in [1]. However, these counterexamples are the result of mathematical constructions. Most of the populations maps considered in the ecological literature satisfy additional conditions, as for example to have negative Schwarzian derivative, which may prevent any destabilizing effects of timing.

Our study leaves several open questions for future research. First, to find what extra conditions are necessary for **Conjecture 1** to hold. Second, **Theorem 1** together with **Proposition 2** guarantee global stability in a strict subset of the  $(r, \gamma)$ -parameter region of asymptotic stability for the positive equilibrium of (4) for the Ricker case (see Fig. 4): we believe that it should be possible to extend our results to enlarge this region of global stability. Finally, we have shown that timing can be stabilizing by itself in the Ricker–Seno model. It would be interesting to provide general conditions for this property to hold in other population models.

**Acknowledgments**

The authors would like to thank the editor and two anonymous referees for their constructive comments. D. Franco and J. Perán were supported by the ETSI Industriales, project 2017-MAT09. D. Franco, J. Perán and J. Segura were supported by the Spanish Ministerio de Economía y Competitividad and FEDER, grant MTM2013-43404-P.

**Appendix**

*The bilinear form N*

Let  $N : \mathbb{R}^3 \times \mathbb{R}^3 \rightarrow \mathbb{R}$  be the bilinear form  $N(\mathbf{v}, \mathbf{w}) = v_1w_3 + w_1v_3 - 3v_2w_2$ .

**Lemma 4.** *If  $\mathbf{u}_0, \mathbf{u}_1 \in \mathbb{R}^3$  satisfy  $N(\mathbf{u}_0, \mathbf{u}_0) < 0$  and  $N(\mathbf{u}_1, \mathbf{u}_1) < 0$ , then the following conditions are equivalent:*

1.  $N(\theta\mathbf{u}_1 + (1 - \theta)\mathbf{u}_0, \theta\mathbf{u}_1 + (1 - \theta)\mathbf{u}_0) < 0$  for all  $\theta \in [0, 1]$ .
2.  $N(\mathbf{u}_0, \mathbf{u}_1) < \sqrt{N(\mathbf{u}_0, \mathbf{u}_0)N(\mathbf{u}_1, \mathbf{u}_1)}$ .

**Proof.** Let us denote  $N_{\alpha\beta} := N(\alpha\mathbf{u}_1 + (1 - \alpha)\mathbf{u}_0, \beta\mathbf{u}_1 + (1 - \beta)\mathbf{u}_0)$  for  $\alpha, \beta \in [0, 1]$ . In particular, with this notation, we have  $N(\mathbf{u}_0, \mathbf{u}_0) = N_{00}$ ,  $N(\mathbf{u}_1, \mathbf{u}_1) = N_{11}$  and  $N(\mathbf{u}_0, \mathbf{u}_1) = N_{01}$ .

Solving  $\frac{dN_{\theta\theta}}{d\theta} = 0$ , we find that its solution is  $\theta = \theta_m := \frac{N_{01} - N_{00}}{2N_{01} - N_{00} - N_{11}}$ . Substituting, we obtain  $N_{\theta_m\theta_m} = \frac{N_{00}N_{11} - N_{01}^2}{N_{00} + N_{11} - 2N_{01}}$ .

Next, we note that for  $\theta_m$  to lie in the interval  $[0, 1]$  the value  $N_{01}$  cannot be between  $N_{00}$  and  $N_{11}$ , that is,

$$\theta_m \in [0, 1] \Leftrightarrow N_{01} \notin (\min\{N_{00}, N_{11}\}, \max\{N_{00}, N_{11}\}).$$

On the other hand, the minimum, the maximum, the arithmetic mean and the geometric mean of  $N_{00}$  and  $N_{11}$  are ordered as follows:

$$\min\{N_{00}, N_{11}\} \leq \frac{N_{00} + N_{11}}{2} \leq -\sqrt{N_{00}N_{11}} \leq \max\{N_{00}, N_{11}\} \leq 0 \leq \sqrt{N_{00}N_{11}}.$$

Thus,  $N_{\theta_m\theta_m} \geq 0$  and  $\theta_m \in [0, 1]$  if and only if  $N_{01} \in [\sqrt{N_{00}N_{11}}, \infty)$ . □

*The polynomial P*

Doing  $z = rx$ , we have

$$\mathbf{u}_0 = \begin{pmatrix} F'_0(x) \\ F''_0(x) \\ F'''_0(x) \end{pmatrix}^T = e^{r-z+z\gamma} (\gamma - 1) \begin{pmatrix} z - z\gamma - 1 \\ r(\gamma - 1)(z - z\gamma - 2) \\ r^2(\gamma - 1)^2(z - z\gamma - 3) \end{pmatrix}^T \text{ and}$$

$$\mathbf{u}_1 = \begin{pmatrix} F_1'(x) \\ F_1''(x) \\ F_1'''(x) \end{pmatrix}^T = e^{r-z}(\gamma - 1) \begin{pmatrix} z - 1 \\ r(2 - z) \\ r^2(z - 3) \end{pmatrix}^T.$$

Therefore,  $\frac{N(\mathbf{u}_0, \mathbf{u}_0)}{[e^{r-z+z\gamma}(\gamma-1)]^2} = r^2(\gamma-1)^2((2\gamma-\gamma^2-1)z^2 + (4-4\gamma)z - 6)$ , and  $\frac{N(\mathbf{u}_1, \mathbf{u}_1)}{[e^{r-z}(\gamma-1)]^2} = -r^2(z^2 - 4z + 6)$ , whereas  $\frac{N(\mathbf{u}_0, \mathbf{u}_1)}{e^{2r-2z+z\gamma}(\gamma-1)^2} = r^2((2\gamma-\gamma^3-1)z^2 + (\gamma^3-6\gamma+4)z + (3\gamma^2+6\gamma-6))$ . Finally, using these expressions, it is not so hard to show that

$$P(z) = \frac{N(\mathbf{u}_0, \mathbf{u}_0)N(\mathbf{u}_1, \mathbf{u}_1) - (N(\mathbf{u}_0, \mathbf{u}_1))^2}{[r^2 e^{2r-2z+z\gamma} (\gamma-1)^2 \gamma]^2}$$

is the quartic polynomial with coefficients given by (9).

## References

- [1] B. Cid, F.M. Hilker, E. Liz, Harvest timing and its population dynamic consequences in a discrete single-species model, *Math. Biosci.* 248 (2014) 78–87.
- [2] E.J. Blomberg, The influence of harvest timing on greater sage-grouse survival: A cautionary perspective, *J. Wildl. Manag.* 79 (5) (2015) 695–703.
- [3] H. Kokko, Optimal and suboptimal use of compensatory responses to harvesting: timing of hunting as an example, *Wildl. Biol.* 7 (3) (2001) 141–150.
- [4] I.I. Ratikainen, J.A. Gill, T.G. Gunnarsson, W.J. Sutherland, H. Kokko, When density dependence is not instantaneous: theoretical developments and management implications, *Ecol. Lett.* 11 (2) (2008) 184–198.
- [5] B.K. Sandercock, E.B. Nilsen, H. Brøseth, H.C. Pedersen, Is hunting mortality additive or compensatory to natural mortality? Effects of experimental harvest on the survival and cause-specific mortality of willow ptarmigan, *J. Animal Ecol.* 80 (1) (2011) 244–258.
- [6] W.M. Getz, R.G. Haight, *Population Harvesting: Demographic Models of Fish, Forest, and Animal Resources*, 27, Princeton University Press, Princeton, 1989.
- [7] H. Seno, A paradox in discrete single species population dynamics with harvesting/thinning, *Math. Biosci.* 214 (1) (2008) 63–69.
- [8] P. Carmona, D. Franco, Control of chaotic behaviour and prevention of extinction using constant proportional feedback, *Nonlinear Anal.: Real W. Appl.* 12 (6) (2011) 3719–3726.
- [9] N.P. Chau, Controlling chaos by periodic proportional pulses, *Phys. Lett. A* 234 (3) (1997) 193–197.
- [10] E. Liz, How to control chaotic behaviour and population size with proportional feedback, *Phys. Lett. A* 374 (5) (2010) 725–728.
- [11] W.E. Ricker, Stock and recruitment, *J. Fish. Res. Board Can.* 11 (5) (1954) 559–623.
- [12] P. Sah, S. Dey, Stabilizing spatially-structured populations through adaptive limiter control, *PLOS ONE* 9 (8) (2014) 1–9.
- [13] E.C. Balreira, S. Elaydi, R. Luis, Local stability implies global stability for the planar Ricker competition model, *Discret. Contin. Dyn. Syst.-Ser. B* 19 (2) (2014) 323–351.
- [14] J. Perán, D. Franco, Global convergence of the second order Ricker equation, *Appl. Math. Lett.* 47 (2015) 47–53.
- [15] B. Ryals, R.J. Sacker, Global stability in the 2D Ricker equation, *J. Differ. Equ. Appl.* 21 (11) (2015) 1068–1081.
- [16] D. Singer, Stable orbits and bifurcation of maps of the interval, *SIAM J. Appl. Math.* 35 (2) (1978) 260–267.
- [17] J. Güémez, M.A. Matias, Control of chaos in unidimensional maps, *Phys. Lett. A* 181 (1) (1993) 29–32.
- [18] H. Seno, Native intra-and inter-specific reactions may cause the paradox of pest control with harvesting, *J. Biol. Dyn.* 4 (3) (2010) 235–247.
- [19] W.C. Clark, *Mathematical Bioeconomics: The Mathematics of Conservation*, 91, John Wiley & Sons, Hoboken, 2010.
- [20] R.M. May, Simple mathematical models with very complicated dynamics, *Nature* 261 (5560) (1976) 459–467.
- [21] E. Braverman, E. Liz, Global stabilization of periodic orbits using a proportional feedback control with pulses, *Nonlinear Dyn.* 67 (4) (2012) 2467–2475.
- [22] M.P. Hassell, Density-dependence in single-species populations, *J. Animal Ecol.* (1975) 283–295.
- [23] D.J. Allwright, Hypergraphic functions and bifurcations in recurrence relations, *SIAM J. Appl. Math.* 34 (4) (1978) 687–691.
- [24] V.J. López, E. Parreño, L.A.S. and negative Schwarzian derivative do not imply G.A.S. in Clark's equation, *J. Dyn. Differ. Equ.* 28 (2) (2016) 339–374.
- [25] R. Irving, *Beyond the Quadratic Formula*, in: Classroom Resource Materials, Mathematical Association of America, Washington, 2013.
- [26] E. Braverman, A. Rodkina, Stabilization of difference equations with noisy proportional feedback control (2016). ArXiv:1606.01970.
- [27] S. Dey, A. Joshi, Stability via asynchrony in drosophila metapopulations with low migration rates, *Science* 312 (5772) (2006) 434–436.
- [28] S.M. Henson, R.F. Costantino, J.M. Cushing, R.A. Desharnais, B. Dennis, A.A. King, Lattice effects observed in chaotic dynamics of experimental populations, *Science* 294 (5542) (2001) 602–605.
- [29] E. Braverman, C. Kelly, A. Rodkina, Stabilisation of difference equations with noisy prediction-based control, *Physica D: Nonlinear Phenom.* 326 (2016) 21–31.
- [30] E. Liz, A. Ruiz-Herrera, The hydra effect, bubbles, and chaos in a simple discrete population model with constant effort harvesting, *J. Math. Biol.* 65 (5) (2012) 997–1016.
- [31] R.J.H. Beverton, S.J. Holt, On the Dynamics of Exploited Fish populations, in: *Fisheries and Food (Series 2)*, Fishery investigations, 19, Ministry of Agriculture, 1957.
- [32] E.S.E. Hafez, Effects of high temperature on reproduction, *Int. J. Biometeorol.* 7 (3) (1964) 223–230.
- [33] A.P. Møller, E. Flensted-Jensen, K. Klarborg, W. Mardal, J.T. Nielsen, Climate change affects the duration of the reproductive season in birds, *J. Animal Ecol.* 79 (4) (2010) 777–784.
- [34] R.A. Taylor, A. White, J.A. Sherratt, How do variations in seasonality affect population cycles? *Proc. Royal Soc. B.* 280 (2013) 20122714.